JACS
JOURNAL OF THE AMERICAN CHEMICAL SOCIETY

COMMUNICATION

pubs.acs.org/JACS

Nanonet-Based Hematite Heteronanostructures for Efficient Solar Water Splitting

Yongjing Lin, Sa Zhou, Stafford W. Sheehan, and Dunwei Wang*

Department of Chemistry, Merkert Chemistry Center, Boston College, Chestnut Hill, Massachusetts 02467, United States

Supporting Information

ABSTRACT: We report the highest external quantum efficiency measured on hematite (α-Fe_2O_3) without intentional doping in a water-splitting environment: 46% at λ = 400 nm. This result was enabled by the introduction of $TiSi_2$ nanonets, which are highly conductive and have suitably high surface areas. The nanonets serve a dual role as a structural support and an efficient charge collector, allowing for maximum photon-to-charge conversion. Without the addition of any oxygen-evolving catalysts, we obtained photocurrents of 1.6 and 2.7 mA/cm^2 at 1.23 and 1.53 V vs RHE, respectively. These results highlight the importance of charge transport in semiconductor-based water splitting, particularly for materials whose performance is limited by poor charge diffusion. Our design introduces material components to provide a dedicated charge-transport pathway, alleviating the reliance on the materials' intrinsic properties, and therefore has the potential to greatly broaden where and how various existing materials can be used in energy-related applications.

Semiconductors hold great promise for high-efficiency solar water splitting as a form of solar energy harvesting and storage. Since the first demonstration using TiO_2,[1] a large number of materials have been studied for this application.[2,3] Among them, hematite (α-Fe_2O_3) stands out for at least two important reasons: (1) its band gap (2.0−2.2 eV) is close to the optimum requirement for a single-junction system, and (2) it consists of two abundant elements and therefore is low-cost and amenable to large-scale implementations.[4−7] Despite intense effort, however, research on using hematite for solar water splitting is progressing at a slow pace because of several challenges presented by the material's intrinsic properties. For instance, the charge-diffusion distance in Fe_2O_3 is notoriously short (on the order of a few to tens of nanometers), making collection of photogenerated charges extremely difficult. Much ongoing effort is focused on addressing this problem by doping Fe_2O_3 to increase the charge-diffusion distance,[4,8] innovating its morphology to improve charge collection,[6,9] or both. Employing a chemical vapor deposition (CVD) protocol, Sivula, Grätzel, and co-workers[7] have been able to achieve photocurrents of 2.3 and 3.0 mA/cm^2 without and with oxygen-evolving catalysts, respectively, at 1.23 V versus a reversible hydrogen electrode (RHE; all potentials appearing hereafter are relative to RHE) on a cauliflower-type hematite nanostructure. In an effort to develop an approach that can be readily and broadly applied to other systems, we have exploited the idea of forming nanoscale heterostructures. By having a dedicated charge-transport pathway, our design enables efficient charge collection. We have shown that this design improves the performance of TiO_2 and WO_3, respectively.[10,11] In this communication, we extend this design principle to hematite and demonstrate that high performance can be achieved on Fe_2O_3 without intentional doping or catalyst decorations.

A key factor enabling our design is our discovery of the $TiSi_2$ nanonet, which exhibits high conductivity and suitably high surface area.[12] As illustrated in Figure 1a, when a thin Fe_2O_3 layer is interfaced with a $TiSi_2$ nanonet, the longest distance from anywhere in the semiconductor to a location where charges can be scavenged (by H_2O oxidation in the solution) or transported (by $TiSi_2$) can be shorter than the charge-diffusion distance, permitting effective charge collection. To actualize the full potential of this design, it is important to synthesize high-quality hematite that is thin and covers the $TiSi_2$ nanonet uniformly. To accomplish this goal, we used an atomic layer deposition (ALD) technique. With $Fe_2(O^tBu)_6$ and H_2O as the Fe and O precursors,[13] respectively, we were able to achieve Fe_2O_3 growth with precise control over the thickness. Postgrowth annealing at 500 °C in O_2 was found to improve the crystallinity of the hematite, as evidenced by structural characterization. More details on the synthesis and postgrowth treatment are available in the Supporting Information (SI). Of importance to our design principles are the requirements that the Fe_2O_3 coating around the $TiSi_2$ nanonet be uniform (Figure 1b) and the interface between Fe_2O_3 and $TiSi_2$ be defect-free (Figure 1c). This allows for charge transfer from Fe_2O_3 to $TiSi_2$ without significant impedance, as confirmed by our electrochemical impedance spectroscopy (EIS) measurements (see Figure 3, the details of which will be discussed later in this communication). We note that although Fe_2O_3 synthesis by ALD has been reported previously,[13,14] it has not been studied for water-splitting reactions. The present work is therefore new and significant.

After their preparation, the $Fe_2O_3/TiSi_2$ heterostructures (Fe_2O_3 thickness 25 nm)[15] were made into electrodes in a fashion similar to that reported by us previously[10] (also see the SI). The electrolyte was NaOH (1 M); the counter electrode was a Pt mesh, and the reference electrode was Hg/HgO in NaOH (1 M). The light source for all of the data presented in this communication, including that for the monochromic light, was a solar simulator (Oriel model 96000) whose intensity was adjusted to 100 mW/cm^2 using with an AM 1.5 filter). In the dark, no substantial current (<10 μA/cm^2) was observed up to 1.60 V, indicating that a band bending was formed between Fe_2O_3 and the electrolyte, resulting in a built-in field that prevented significant charge transfer from the

Received: December 9, 2010
Published: February 9, 2011

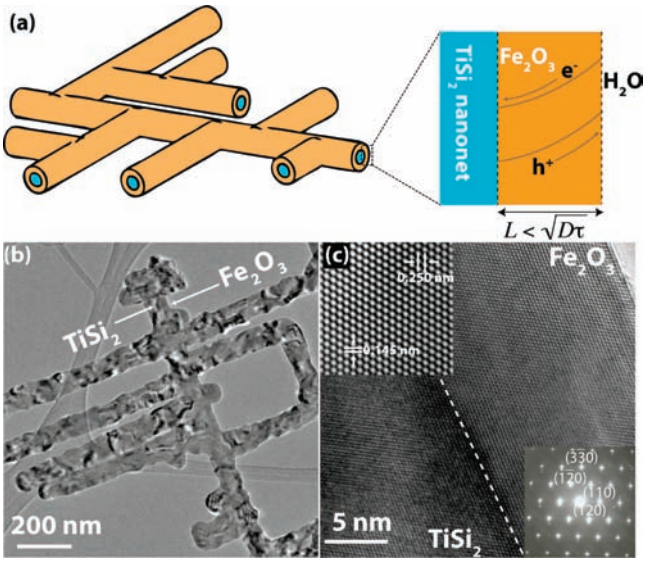

Figure 1. (a) Schematic illustration of the design principle, which involves the use of a highly conductive $TiSi_2$ nanonet as an effective charge collector. The electronic band structure is shown in the enlarged cross-sectional view. Efficient charge collection is achieved when the hematite thickness is smaller than the charge-diffusion distance. (b) Low-magnification transmission electron microscopy (TEM) image showing the structural complexity of a typical heteronanostructure and its $TiSi_2$ core/hematite shell nature. (c) High-resolution (HR) TEM data. A dashed line has been added at the interface as a guide to the eyes. Insets: (left) lattice-fringe-resolved HRTEM image showing the hematite lattice spacings for (110) (0.250 nm) and ($\bar{3}30$) (0.145 nm); (right) electron diffraction pattern of hematite.

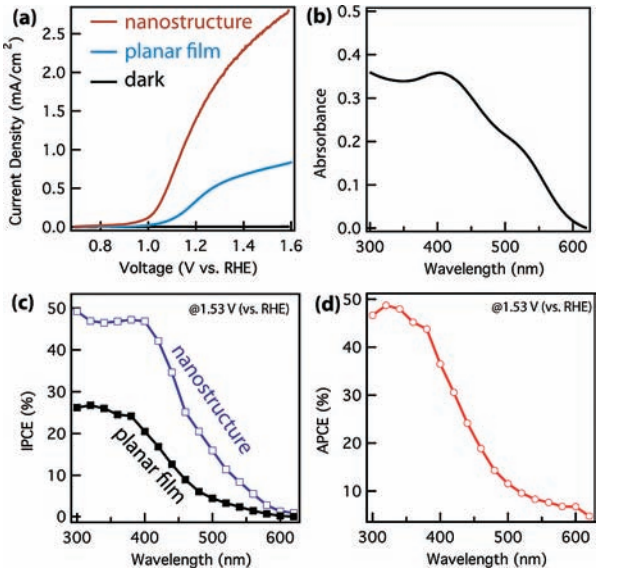

Figure 2. Photoelectrochemical (PEC) properties of $TiSi_2/Fe_2O_3$ heteronanostructures. (a) Characteristic PEC data of an $Fe_2O_3/TiSi_2$ heteronanostructure and a planar hematite film. (b) Absorption spectrum of the Fe_2O_3 film (see the SI for more experimental details). (c) Comparison of the external quantum efficiencies (IPCEs) of Fe_2O_3 with and without $TiSi_2$ nanonets (measured at V = 1.53 V vs RHE). The introduction of a highly conductive component increases the IPCE significantly. (d) Internal quantum efficiency (APCE) of planar Fe_2O_3 on FTO-coated glass, calculated from the IPCE and the absorption spectrum (see the SI).

solution to the semiconductor (or vice versa). In contrast, a large current was measured when the electrode was illuminated (2.7 mA/cm^2 at 1.53 V and 1.6 mA/cm^2 at 1.23 V; Figure 2a). Importantly these measurements were performed on Fe_2O_3 without any cocatalysts. Although these values are lower than those reported in ref 7, they are higher than those in most other existing reports, and to the best of our knowledge, they are the highest measured on Fe_2O_3 without intentional doping.[16] This result provides evidence that the heteronanostructure design is an alternative to doping for improvement of charge collection. Further increases in the photocurrent should be possible by, for example, using cocatalysts to lower the onset potential (presently ~0.90 V).[3,7,17]

The incident photon-to-charge conversion efficiencies (IPCEs) of the $Fe_2O_3/TiSi_2$ heterostructure and a planar hematite film were measured as a function of wavelength, and the data are plotted in Figure 2c. We emphasize the difference between the performance of the heteronanostructures and that of the planar films, the former being nearly twice as high as the latter. The highest IPCE measured for the nanostructure (46% at λ = 400 nm) is equal to or better than those in existing reports. That it is significantly lower than those of TiO_2 or WO_3 (typically >80%) suggests that there is plenty of room for improvement in either light absorption, charge collection, or both. To understand which factor is more important, we examined the adsorbed photon-to-charge conversion efficiency (APCE) of planar Fe_2O_3 (25 nm) grown on fluorinated tin oxide (FTO)-coated glass. As shown in Figure 2d, the APCE of the Fe_2O_3 thin film is on the same level as the IPCE of the $Fe_2O_3/TiSi_2$ heterostructure. Lower APCEs were measured on thicker Fe_2O_3 films, presumably because of the poorer charge collection. Our ability to prepare ultrathin crystalline Fe_2O_3 allowed us to measure the internal quantum efficiencies without being confounded by poor charge collection. This result further reveals that even when only the absorbed photons (Figure 2b) were considered, a relatively low (<50%) quantum efficiency was measured, and the efficiency was especially low in the long-wavelength range, where the excited electrons have lower energy (e.g., ~16% at 500 nm). This finding is in line with current literature reports that the quantum yield for converting photons with energies close to the Fe_2O_3 band edge is low. We note that this issue may be addressed by doping and that our design and the doping strategy are not exclusive to each other because there are no fundamental reasons that would prevent us from taking advantage of doped Fe_2O_3. We are currently in the process of combining doped Fe_2O_3 with $TiSi_2$ nanonets and examining the resulting materials. Nonetheless, it is important to point out that the data in Figure 2 also prove the power of the heterostructure design, which exhibits the highest IPCE measured on undoped Fe_2O_3.

Because a low impedance across the interface between Fe_2O_3 and $TiSi_2$ is critical for the realization of the nanonet-based design, we carried out detailed study of this interface using EIS in the dark under steady-state conditions. Briefly, a potential (varying from 0.8 to 2.1 V) was applied, and the system was allowed to equilibrate for 5 min. Afterward, an alternating-current (AC) perturbation of the applied potential (with a magnitude of 5 mV and frequencies changing from 100 000 to 1 Hz) was exerted, and the impedance changes in response to the perturbation were measured. A typical set of data (at 1.9 V) is plotted in Figure 3a in the form of a Nyquist plot. Following protocols reported by others and us,[18] we then employed an equivalent electrical circuit to analyze the data. This technique allowed us to single out two important elements of the system in a quantitative fashion: the series resistance (including that between $TiSi_2$ and Fe_2O_3) and the capacitance of the depletion region within

dx.doi.org/10.1021/ja110741z |J. Am. Chem. Soc. 2011, 133, 2398–2401

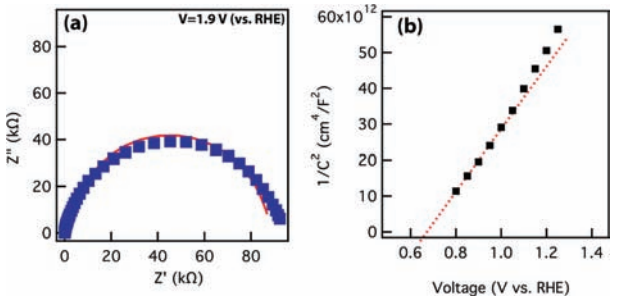

Figure 3. Impedance studies revealing quantitative information on the intrinsic properties of the heteronanostructures. (a) Nyquist plot of the impedance measurements at 1.9 V vs RHE. The frequency varied from 10^5 Hz (far left) to 1 Hz (far right). Z' and Z'' are the real and imaginary parts of the impedance, respectively. Blue squares represent the experimental data, and the red curve shows simulated data obtained using equivalent circuits. (b) Mott−Schottky plot generated using the capacitance values derived from the EIS data fitting, from which the flatband potential and charge-carrier concentration were extracted.

Fe_2O_3 (Figure 3b). The variation of the measured series resistance (~8 Ω) as a function of the applied potential was minimal, suggesting efficient charge transfer from Fe_2O_3 to the $TiSi_2$ nanonet and then to the charge collector. The measured depletion-region capacitance, on the other hand, decreased monotonically with increasing potential as described by the Mott−Schottky (M−S) relation, fitting to which (between 0.8 and 1.1 V vs RHE) yielded two important properties of the Fe_2O_3: the flatband potential (V_{fb} = 0.67 V) and the charge-carrier concentration (2.0×10^{16} carriers/cm^3) (more details about these experiments and the data analysis are provided in the SI).[19] Alternatively, the M−S plot could have been obtained by directly measuring the capacitance of the system. However, because of the complexities of the semiconductor−electrolyte interfaces, this approach failed to yield meaningful values of V_{fb} and the carrier concentration. We note that the measured V_{fb} falls in the relevant range that has been reported in the literature but is higher than V_{fb} values for Fe_2O_3 produced by Sivula, Grätzel, and co-workers.[7] The difference may be a result of the low carrier concentration of our material, which also indicates the purity of the ALD-produced Fe_2O_3 coating. We also note that Hamann et al.[15b] recently reported that the M−S method may not be applicable to structures other than planar ones. The quantitative information reported here nonetheless permits comparison with existing literature reports. Future studies will be focused on improving the performance of the heterostructures by utilizing doped Fe_2O_3 as well as reducing the surface overpotential through the introduction of cocatalysts.

In conclusion, research on using hematite to absorb solar light and split water is moving at a slow pace despite the positive prospects arising from its suitable band gap and low cost, and the limiting factor has been the intrinsic physical and chemical properties of this material. We proposed to meet the challenge by introducing the $TiSi_2$ nanonet as a dedicated charge transporter that should improve the charge collection and thus should have the potential to make solar water splitting practical. A record-high photocurrent of 2.7 mA/cm^2 was measured on undoped Fe_2O_3; the quantum efficiency measurements (46% at λ = 400 nm) indicated that by this approach we approached the maximum limit of what can be measured on Fe_2O_3 without intentional doping. Future studies will be focused on improving the collection of charges generated by long-wavelength photons close to the band-gap edge by doping as well as adding cocatalysts.

■ ASSOCIATED CONTENT

Supporting Information. Synthesis of heteronanostructures, XRD patterns, XPS spectra, and optical and electrochemical characterization details. This material is available free of charge via the Internet at http://pubs.acs.org.

■ AUTHOR INFORMATION

Corresponding Author
dunwei.wang@bc.edu

■ ACKNOWLEDGMENT

This research was supported by Boston College. We thank G. Yuan for insightful discussions and D. Wang and H. Wang of Boston College and H. Lin of Harvard University for technical assistance.

■ REFERENCES

(1) Fujishima, A.; Honda, K. *Nature* **1972**, *238*, 37–38.
(2) (a) Grimes, C. A.; Varghese, O. K.; Ranjan, S. *Light, Water, Hydrogen: The Solar Generation of Hydrogen by Water Photoelectrolysis*; Springer: New York, 2008. (b) Bak, T.; Nowotny, J.; Rekas, M.; Sorrell, C. C. *Int. J. Hydrogen Energy* **2002**, *27*, 991–1022. (c) Kudo, A.; Miseki, Y. *Chem. Soc. Rev.* **2009**, *38*, 253–278.
(3) Youngblood, W. J.; Lee, S. H. A.; Maeda, K.; Mallouk, T. E. *Acc. Chem. Res.* **2009**, *42*, 1966–1973.
(4) Kennedy, J. H.; Frese, J. *J. Electrochem. Soc.* **1978**, *125*, 709–714.
(5) (a) Dare-Edwards, M.; Goodenough, J.; Hamnett, A.; Trevellick, P. *J. Chem. Soc., Faraday Trans. 1* **1983**, *79*, 2027–2041. (b) Khan, S. U. M.; Akikusa, J. *J. Phys. Chem. B* **1999**, *103*, 7184–7189. (c) Kay, A.; Cesar, I.; Grätzel, M. *J. Am. Chem. Soc.* **2006**, *128*, 15714–15721.
(6) LaTempa, T. J.; Feng, X.; Paulose, M.; Grimes, C. A. *J. Phys. Chem. C* **2009**, *113*, 16293–16298.
(7) Tilley, S. D.; Cornuz, M.; Sivula, K.; Grätzel, M. *Angew. Chem., Int. Ed.* **2010**, *49*, 6405–6408.
(8) (a) Cesar, I.; Kay, A.; Gonzalez Martinez, J. A.; Grätzel, M. *J. Am. Chem. Soc.* **2006**, *128*, 4582–4583. (b) Glasscock, J. A.; Barnes, P. R. F.; Plumb, I. C.; Savvides, N. *J. Phys. Chem. C* **2007**, *111*, 16477–16488. (c) Hu, Y.-S.; Kleiman-Shwarsctein, A.; Forman, A. J.; Hazen, D.; Park, J.-N.; McFarland, E. W. *Chem. Mater.* **2008**, *20*, 3803–3805. (d) Kleiman-Shwarsctein, A.; Hu, Y.-S.; Forman, A. J.; Stucky, G. D.; McFarland, E. W. *J. Phys. Chem. C* **2008**, *112*, 15900–15907. (e) Saremi-Yarahmadi, S.; Wijayantha, K. G. U.; Tahir, A. A.; Vaidhyanathan, B. *J. Phys. Chem. C* **2009**, *113*, 4768–4778. (f) Jang, J. S.; Lee, J.; Ye, H.; Fan, F.-R. F.; Bard, A. J. *J. Phys. Chem. C* **2009**, *113*, 6719–6724.
(9) (a) Beermann, N.; Vayssieres, L.; Lindquist, S.-E.; Hagfeldt, A. *J. Electrochem. Soc.* **2000**, *147*, 2456–2461. (b) Mathur, S.; Veith, M.; Sivakov, V.; Shen, H.; Huch, V.; Hartmann, U.; Gao, H. B. *Chem. Vap. Deposition* **2002**, *8*, 277–283. (c) Lindgren, T.; Wang, H.; Beermann, N.; Vayssieres, L.; Hagfeldt, A.; Lindquist, S.-E. *Sol. Energy Mater. Sol. Cells* **2002**, *71*, 231–243. (d) Mohapatra, S. K.; John, S. E.; Banerjee, S.; Misra, M. *Chem. Mater.* **2009**, *21*, 3048–3055. (e) Cesar, I.; Sivula, K.; Kay, A.; Zboril, R.; Grätzel, M. *J. Phys. Chem. C* **2009**, *113*, 772–782. (f) Mao, A.; Han, G. Y.; Park, J. H. *J. Mater. Chem.* **2010**, *20*, 2247–2250. (g) Brillet, J.; Grätzel, M.; Sivula, K. *Nano Lett.* **2010**, *10*, 4155–4160.
(10) Lin, Y.; Zhou, S.; Liu, X.; Sheehan, S.; Wang, D. *J. Am. Chem. Soc.* **2009**, *131*, 2772–2773.
(11) Liu, R.; Lin, Y. J.; Chou, L.-Y.; Sheehan, S. W.; He, W.; Zhang, F.; Hou, H. J. M.; Wang, D. W. *Angew. Chem., Int. Ed.* **2011**, *50*, 499–502.
(12) (a) Zhou, S.; Liu, X. H.; Lin, Y. J.; Wang, D. W. *Angew. Chem., Int. Ed.* **2008**, *47*, 7681–7684. (b) Zhou, S.; Liu, X.; Lin, Y.; Wang, D. *Chem. Mater.* **2009**, *21*, 1023–1027.
(13) Bachmann, J.; Jing, J.; Knez, M.; Barth, S.; Shen, H.; Mathur, S.; Gosele, U.; Nielsch, K. *J. Am. Chem. Soc.* **2007**, *129*, 9554–9555.

(14) Lie, M.; Fjellvag, H.; Kjekshus, A. *Thin Solid Films* **2005**, *488*, 74–81.

(15) (a) As in ref 10, we also studied the effect of hematite thickness. Lower performance was observed for thicker or thinner films. More study is necessary to fully understand how the PEC performance depends on hematite thickness. (b) During the review process for this paper, a relevant paper was published: Klahr, B. M.; Martinson, A. B. F.; Hamann, T. W. *Langmuir* **2011**, *27*, 461–468.

(16) Tahir, A. A.; Wijayantha, K. G. U.; Saremi-Yarahmadi, S.; Mazhar, M.; McKee, V. *Chem. Mater.* **2009**, *21*, 3763–3772.

(17) (a) Zhong, D. K.; Sun, J.; Inumaru, H.; Gamelin, D. R. *J. Am. Chem. Soc.* **2009**, *131*, 6086–6087. (b) Zhong, D. K.; Gamelin, D. R. *J. Am. Chem. Soc.* **2010**, *132*, 4202–4207.

(18) (a) Zhou, S.; Wang, D. W. *ACS Nano* **2010**, *4*, 7014–7020.(b) Yuan, G.; Aruda, K.; Zhou, S.; Levine, A.; Xie, J.; Wang, D. *Angew. Chem., Int. Ed.* [Online early access]. DOI: 10.1002/anie.201006617. Published Online: Feb 2, 2011.

(19) Kennedy, J. H.; Frese, K. W. J. *J. Electrochem. Soc.* **1978**, *125*, 723–726.